Appl Phys A (2008) 93: 901–905
DOI 10.1007/s00339-008-4751-4

Applied Physics A
Materials Science & Processing

Measurements of cavitation bubble dynamics based on a beam-deflection probe

Peter Gregorčič · Rok Petkovšek · Janez Možina · Griša Močnik

Received: 12 October 2007 / Accepted: 4 March 2008 / Published online: 21 June 2008

Abstract We present an optodynamic measurement of a laser-induced cavitation bubble and its oscillations based on a scanning technique using a laser beam-deflection probe. The deflection of the beam was detected with a fast quadrant photodiode which was built into the optical probe. The applied experimental setup enabled us to carry out one- or two-dimensional scanning of the cavitation bubble, automatic control of the experiment, data acquisition and data processing. Shadow photography was used as a comparative method during the experiments.

PACS 42.62.-b · 47.40.-x · 47.55.dd

1 Introduction

Cavitation bubbles play an important role in many fields. They deserve a great deal of attention in ocular microsurgery, where Q-switched lasers with nanosecond pulse durations are commonly used to disrupt tissue in procedures such as secondary cataract removal [1]. Understanding the cavitation bubble and the pressure front development, their dynamics and their propagation is important for avoiding adverse effects on the eye during ophthalmic procedures based on laser surgery [2, 3]. Furthermore, cavitation bubbles are interesting for individual cell micromanipulation [4]. Some studies are also related to biomedicine, where the microbubble cavitation is used to enhance membrane permeabilization and molecular uptake (sonoporation) [5].

When a high-intensity laser pulse is focused into a liquid, plasma is formed due to optical breakdown [6]. Explosive expansion of plasma is followed by shock wave emission and the development of a cavitation bubble. In such a process, the optical energy of the laser pulse is converted into the mechanical energy of the shock wave and cavitation bubble through an optodynamic conversion. These two phenomena can be detected by methods such as shadow photography [7, 8] or laser beam-deflection probe (BDP) [9–13]. Both methods require a good repeatability of the measuring process. The main difference between BDP and shadow photography is as follows. With BDP, one can observe all of the bubble's dynamics at one point in space. This means that we can obtain information on all the expansions, collapses, and shock waves from the BDP signal. Shadow photography enables two-dimensional measurements from a single shot. Therefore, BDP scanning requires probe-beam position shifting relative to the breakdown region, while bubble dynamics measurements based on shadow photography require exposure-time delaying relative to the occurrence of the breakdown. By using a scanning procedure the dynamic behavior in 1D or 2D of shock wave or bubble can be measured with BDP [10], but in the case of 2D measurements the shadow photography is more appropriate, since a smaller number of measurements is necessary. On the other hand, BDP is well suited for the investigation of parameter dependencies, such as the bubble's oscillation time in dependence of the distance between the bubble's center and boundary [14]. Furthermore, from a single shot, the collapse times for all bubble oscillations can be obtained [13] and, by using the Rayleigh formula [15], bubble oscillations radii can be calculated.

P. Gregorčič (✉) · R. Petkovšek · J. Možina · G. Močnik
Faculty of Mechanical Engineering, University of Ljubljana, Aškerčeva 6, 1000 Ljubljana, Slovenia
e-mail: peter.gregorcic@fs.uni-lj.si

G. Močnik
Optotek d.o.o., Stegne 13a, 1000 Ljubljana, Slovenia

We present here an optodynamic measurement of the laser-induced cavitation bubble and its oscillations based on a scanning technique using BDP. For data verification reasons, we simultaneously employed shadow photography during our experiments. The main goal of our study was to obtain measurements of the dynamics for the bubble oscillations using a laser beam-deflection probe and to compare them with shadow photography measurements. Measurements were done in an infinite liquid as well as in the vicinity of the rigid boundary. It is well known that a bubble collapsing in an infinite liquid is almost spherical. On the other hand, a cavitation bubble developed near a rigid boundary results in an asymmetrical collapse [16–18]. Under suitable conditions, the deformation during the collapse near a rigid boundary results in the generation of a liquid jet, which is directed toward the wall [16].

2 Experimental setup

A sketch of the experimental setup is shown in Fig. 1. We employed a similar setup in our previous work [13]. The breakdown was induced by an infrared, 1064 nm Q-switched Nd:YAG laser, designed for ocular photodisruption. Pulses with energies of 8.6 mJ and a duration 7 ns were focused into a vessel with deionized water. The NA of the focusing optics of the laser beam was 0.2, which is a typical value in laser systems for optical photodisruption.

We measured the cavitation bubble's wall time-of-flight with the beam-deflection probe. As a probe beam, a He–Ne laser with a beam waist radius ∼3 μm was used. When a cavitation bubble crosses the path of the probe beam, the beam is deflected due to the refractive index gradient [12, 19]. These deflections were detected with a quadrant photo-diode. A detailed description of the beam-deflection probe's signal resulting from the pressure front and a cavitation bubble is presented elsewhere [12, 13]. BDP measurements presented in this paper were performed by scanning in the horizontal direction, i.e., perpendicular to the optical axes of the breakdown beam (from the left to the right; see Fig. 1) for the case of a bubble oscillating in an infinite liquid. At the start of each measurement, the probe beam was placed into the center of shock wave or bubble. The center was defined by the time of flight of a shock wave as follows. The probe beam was first placed approximately 1 mm above the breakdown point, and the time of flight for the shock wave was measured. Then the probe beam was placed approximately 1 mm below the breakdown point and the time of flight of the shock wave was determined. From these two times, the center of the optodynamic source was determined. The same method was used in the horizontal direction. In the case of a bubble oscillating near a rigid boundary, measurements were performed by vertical scanning (from the top to the bottom, see Fig. 1). The positioning system enabling 2D scanning was controlled by two stepper motors. All measurements were performed in steps of 30 μm.

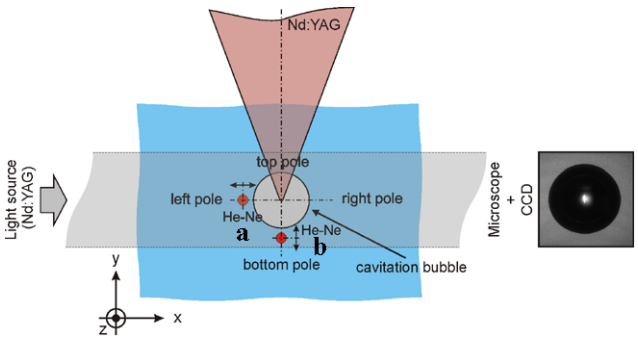

Fig. 1 Experimental setup. The breakdown was induced by a Nd:YAG laser pulse focused into a container with deionized water. The laser pulse with a duration of 7 ns had an energy $E_L = 8.6$ mJ. A He–Ne laser was used as a probe beam. BDP scanning was performed in the horizontal (position **a**) and vertical (position **b**) direction. Shadow photography was employed simultaneously during the experiments. A Nd:YAG laser with a pulse duration of 7 ns was used as a light source for this

The shadow photography was employed simultaneously during our experiments in order to compare the data of the measurement. Since shadow photography needs short exposure times to ensure an appropriate time resolution, a pulsed laser or plasma discharge lamps should be employed as the light source. We used a Q-switched laser with pulse duration 7 ns. The image was captured using a microscope equipped with a CCD camera.

3 Results and discussion

A typical series of signals showing the spreading of a cavitation bubble near a rigid boundary are shown in Fig. 2. The signals show the difference between the photocurrent in left–right or up–down segments. A more detailed description of the signal provided by the quadrant photodiode can be found in [12]. The boundary was placed 3.3 mm ($\gamma \sim 2.1$) below the breakdown region corresponding to the origin point of the bubble. Here, γ is a dimensionless distance, defined as $\gamma = s/R$ [16], where R is the maximum radius of the bubble and s is the distance between the bubble's center and boundary. Scanning was performed in the vertical direction, i.e., parallel to the axis of the breakdown laser. Each signal corresponds to the particular position of the probe beam (y-axis). The first spike shows the shock wave caused by laser-induced breakdown. The following two peaks show the bubble during its expansion and collapse, respectively. In the case when the probe beam is positioned exactly at the maximum radius of the bubble, these two peaks merge into one. This phenomenon can be seen in the first signal from the top. During scanning, the signal

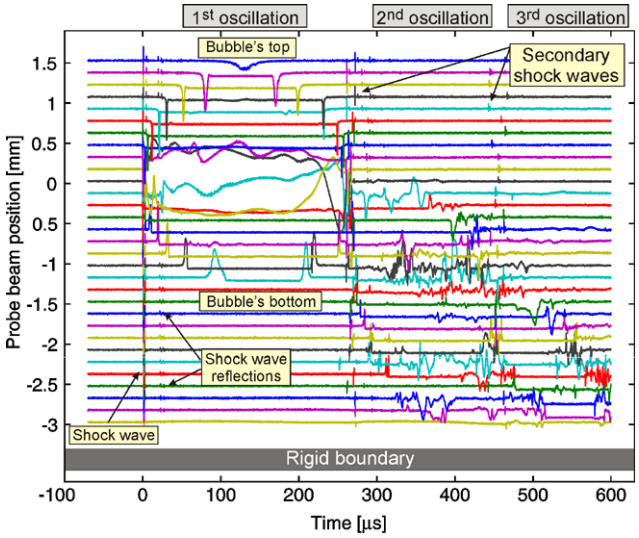

Fig. 2 Typical signal series of BDP vertical scanning. A cavitation bubble was oscillating near a rigid boundary, positioned 3.3 mm ($\gamma \sim 2.1$) below the breakdown region corresponding to the origin point of the bubble. The bubble's first three oscillations as well as peaks showing the first shock wave, induced by optical breakdown and secondary shock waves, caused by bubble collapses, are clearly visible

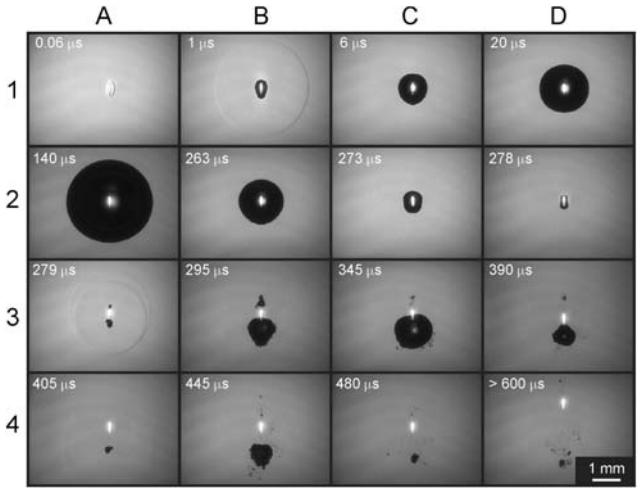

Fig. 3 Typical images of cavitation bubble dynamics in an infinite liquid made by shadow photography. The laser pulse enters from the top of each frame. The *bright spot* in the center shows light radiated from the plasma, while the *black area* on the bright background shows the cavitation bubble. A shock wave is visible as a "ring" surrounding the plasma and the bubble. The scale is shown in frame D4

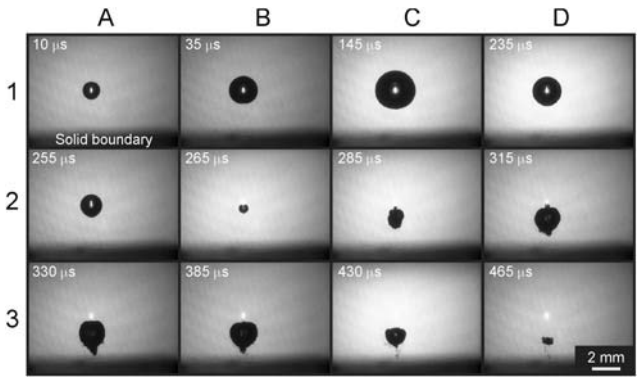

Fig. 4 Images of an oscillating bubble near a rigid boundary. The boundary was placed 3.3 mm ($\gamma \sim 2.1$) below the breakdown center. The liquid jet is visible from C2 to D3. The scale is shown in frame D3

changes polarity when the probe's beam crosses the breakdown region (probe beam position 0). The first oscillation is visible from signals between 0 and ~270 μs. After the first collapse, the bubble rebounds and the process repeats itself in the second (between ~270 and ~470 μs) and third (between ~470 and ~600 μs) oscillations. Secondary shock waves, emitted after every collapse, are also visible from BDP signals. The symmetry was lost in the presence of the rigid boundary, which also caused a migration of the bubble toward the wall.

Figure 3 shows some typical images of a bubble oscillating in infinite liquid as obtained by shadow photography (which we used as a reference method). The bright spot in the center corresponds to the light radiated from the plasma. The shock wave is visible on frame B1 as a ring surrounding the plasma and the bubble. The cavitation bubble, visible as a black area on the bright background, expanded to its maximum radius at $t \sim 140$ μs (frame A2) and then started to collapse. At an early stage of the spreading the cavitation bubble is slightly conical (see frame B1). This agrees with the shape of the laser-induced plasma, reported elsewhere [20, 21]. This non-spherical nature of the initial bubble behavior becomes remarkable at the first bubble collapse (see images C2, D2). At time $t \sim 280$ μs (frame A3) one can see the secondary shock wave emitted as a result of the bubble's collapse. During the first collapse, the bubble splits into two parts (see images A3–D3). This split is the result of the non-spherical bubble shape [22]. Later, the bubble expanded to its maximum radius of the second oscillation (frame C3). After the end of the oscillations, the gas bubbles remained close to the breakdown region for a few seconds after the breakdown [20] and are visible in the last frame (D4) of Fig. 3.

Figure 4 shows some typical images captured near a rigid boundary. The distance between the rigid boundary and the center of the bubble was $s = 3.3$ mm ($\gamma \sim 2.1$). The rigid boundary was positioned below the bubble. When a bubble collapses in the vicinity of the rigid boundary, the boundary hinders the flow of fluid toward the bubble. As a result, a low-pressure region develops between the bubble and the boundary [23], and this leads to a difference in the pressure between the liquid below and above the bubble, causing a strong acceleration of the bubble's upper wall. As a result, a liquid jet is formed and directed toward the rigid boundary. The jet hits the bubble's opposite wall in the final stage of the collapse and penetrates the bubble during the collapse

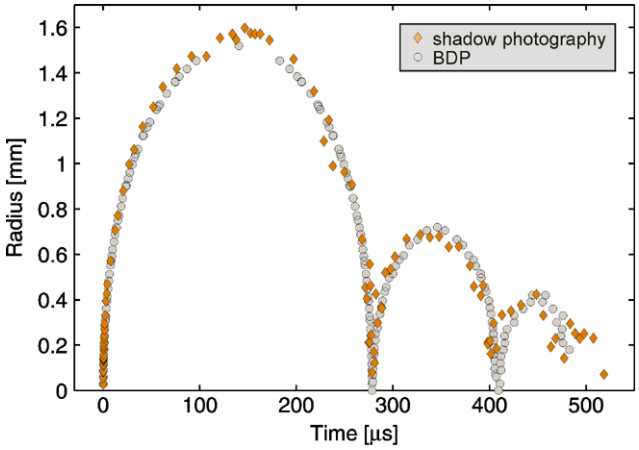

Fig. 5 Bubble radius versus time for the bubble in an infinite liquid. Comparison between the results obtained from the BDP (*circles*) and shadow photography (*deltoids*) shows excellent agreement of the methods. In the case of BDP measurements the data were processed by the method for reducing the measurement noise during the BDP scanning procedure [13]

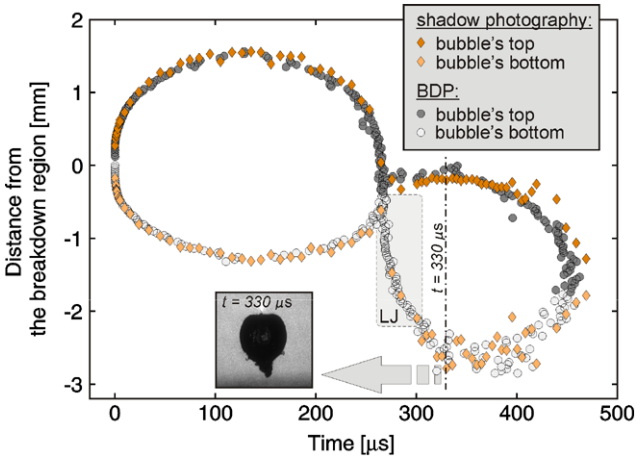

Fig. 6 The movement of the top and the bottom of the bubble oscillating near a rigid boundary. The boundary was placed 3.3 mm ($\gamma \sim 2.1$) below the breakdown region. Comparison between the results obtained from the BDP (*circles*) and shadow photography (*deltoids*) shows excellent agreement of the methods. A rectangle (LJ) marks the development of the liquid jet. The image shows the liquid jet at its maximum size

and rebound [17]. From frames D2–C3 in Fig. 4, we can see that this becomes visible during the second oscillation.

A quantitative evolution of the measured cavitation bubble's radius in an infinite liquid is shown in Fig. 5. The vertical axis represents the bubble radius. In the case of the results obtained by BDP (circles), the bubble radius was obtained from the position of the probe relative to the breakdown site during the scanning procedure. The data were processed by the method for reducing the measurement noise during the BDP scanning procedure [13]. This improved technique uses a unique property of BDP: all the cavitation bubble's expansions, collapses and shock waves can be obtained from a single shot. Comparison with shadow photography measurements (deltoids) confirms an excellent agreement between methods, where the scatter of the data obtained by the BDP is smaller than with shadow photography, since in the first case the method for reducing the measurement noise was used. A detailed description of the method can be found in [13].

A quantitative evolution of the top and the bottom of the bubble near a rigid boundary is shown in Fig. 6. The vertical axis shows the distance relative to the breakdown region. Here, a positive sign on the vertical axis corresponds to the distance above the initial position of the bubble (i.e., breakdown region), while a negative sign corresponds to the distances below the breakdown region. In the case of the BDP measurements (circles), the bubble's top and bottom were distinguished in the BDP signals from the polarization of the peaks. Each point is the average of four measurements. The slope of the graph shows the velocities of the bubble's top and the bottom. Frames C2–C3 in Fig. 4 show that the jet is formed on the bottom of the bubble after the rebound. In Fig. 6, a liquid jet is visible as an increase in the velocity of the bubble's bottom (between ~270 and ~300 µs) and is marked by a rectangle (LJ). Also in the aspect of bubble which oscillates near a rigid boundary the results of the shadow photography measurements (deltoids) agree with the results obtained by beam-deflection probe measurements. Also in this case the scatter of the data obtained by the BDP is smaller than with shadow photography. The main reason is that more repetitions were done by BDP, since the employed system enabled automatic acquisition of large amounts of data.

4 Conclusion

We have presented optodynamic measurements of the laser-induced cavitation bubble and its oscillations, based on a scanning technique by using laser beam-deflection probe. With BDP, we measured a bubble oscillating in an infinite liquid as well as a bubble oscillating near a rigid boundary. In the latter case, asymmetrical collapse was visible. The shadow photography was simultaneously employed during experiments for data verification reasons. Comparison of the results demonstrated good agreement of both methods. On one hand, the main advantage of the shadow photography is that the whole 2D image is acquired. On the other hand, the main advantage of the BDP is that from the signal, acquired with a single shot, information of collapse times for all bubble oscillations and consequently bubble oscillation radii can be obtained.

References

1. A. Vogel, Phys. Med. Biol. **42**, 895–912 (1997)
2. I. Apitz, A. Vogel, Appl. Phys. A **81**, 329–338 (2005)
3. R. Petkovšek, G. Močnik, J. Možina, Fluid Phase Equilib. **256**, 158–162 (2007)
4. V. Venugopalan, A. Guerra, K. Nahen, A. Vogel, Phys. Rev. Lett. **88**, 078103 (2002)
5. P. Marmottant, S. Hilgenfeldt, Nature **423**, 153–156 (2003)
6. P.K. Kennedy, IEEE J. Quantum Electron. **31**, 2241–2249 (1995)
7. A. Vogel, S. Busch, U. Parlitz, J. Acoust. Soc. Am. **100**, 148–165 (1996)
8. J. Noack, D.X. Hammer, G.D. Noojin, B.A. Rockwell, A. Vogel, J. Appl. Phys. **83**, 7488–7495 (1998)
9. A. Vogel, W. Lauterborn, J. Acoust. Soc. Am. **84**, 719–731 (1988)
10. R. Petkovšek, J. Možina, G. Močnik, Opt. Express **13**, 4107–4112 (2005)
11. R. Zhao, R.Q. Xu, Z.H. Shen, J. Lu, X.W. Ni, Opt. Laser Technol. **39**, 968–972 (2007)
12. R. Petkovšek, P. Gregorčič, J. Možina, Meas. Sci. Technol. **18**, 2972–2978 (2007)
13. R. Petkovšek, P. Gregorčič, J. Appl. Phys. **102**, 044909 (2007)
14. P. Gregorčič, R. Petkovšek, J. Možina, J. Appl. Phys. **102**, 094904 (2007)
15. L. Rayleigh, Philos. Mag. **34**, 94–98 (1917)
16. Y. Tomita, A. Shima, J. Fluid Mech. **169**, 535–564 (1986)
17. A. Vogel, W. Lauterborn, R. Timm, J. Fluid Mech. **206**, 299–338 (1989)
18. A. Philipp, W. Lauterborn, J. Fluid Mech. **361**, 75–116 (1998)
19. J. Diaci, Rev. Sci. Instrum. **63**, 5306–5310 (1992)
20. A. Vogel, K. Nahen, D. Theisen, J. Noack, IEEE J. Sel. Top. Quantum Electron. **2**, 847–860 (1996)
21. J. Noack, D.X. Hammer, G.D. Noojin, B.A. Rockwell, A. Vogel, J. Appl. Phys. **83**, 7488–7495 (1998)
22. E.A. Brujan, K. Nahen, P. Schmidt, A. Vogel, J. Fluid Mech. **433**, 251–281 (2001)
23. A. Vogel, *Optical Breakdown in Water and Ocular Media, and Its Use for Intraocular Photodisruption* (Shaker, Aachen, 2001)